Dual-modal three-dimensional imaging of single cells with isometric high resolution using an optical projection tomography microscope

Qin Miao
University of Washington
Department of Bioengineering
204 Fluke Hall
Seattle, Washington 98195

J. Richard Rahn
Anna Tourovskaia
Michael G. Meyer
Thomas Neumann
Alan C. Nelson
Vision Gate Inc.
1509 56th Avenue Court North West
Gig Harbor, Washington 98335

Eric J. Seibel
University of Washington
Dept. of Mechanical Engineering
P.O. Box 352600
Seattle, Washington 98195

Abstract. The practice of clinical cytology relies on bright-field microscopy using absorption dyes like hematoxylin and eosin in the transmission mode, while the practice of research microscopy relies on fluorescence microscopy in the epi-illumination mode. The optical projection tomography microscope is an optical microscope that can generate 3-D images of single cells with isometric high resolution both in absorption and fluorescence mode. Although the depth of field of the microscope objective is in the submicron range, it can be extended by scanning the objective's focal plane. The extended depth of field image is similar to a projection in a conventional x-ray computed tomography. Cells suspended in optical gel flow through a custom-designed microcapillary. Multiple pseudoprojection images are taken by rotating the microcapillary. After these pseudoprojection images are further aligned, computed tomography methods are applied to create 3-D reconstruction. 3-D reconstructed images of single cells are shown in both absorption and fluorescence mode. Fluorescence spatial resolution is measured at 0.35 μm in both axial and lateral dimensions. Since fluorescence and absorption images are taken in two different rotations, mechanical error may cause misalignment of 3-D images. This mechanical error is estimated to be within the resolution of the system. [DOI: 10.1117/1.3275470]

Keywords: multimodal microscopy; three-dimensional microscopy; tomographic imaging.

Paper 09148PRR received Apr. 15, 2009; revised manuscript received Oct. 15, 2009; accepted for publication Oct. 15, 2009; published online Dec. 21, 2009. This paper is a revision of a paper presented at the SPIE conference on Biomedical Applications in Molecular, Structural, and Functional Imaging, February 2009, Lake Buena Vista, Florida. The paper presented there appears (unrefereed) in SPIE Proceedings Vol. 7262.

1 Introduction

3-D imaging is in increasing demand in current biological research. The 3-D images are usually acquired by taking a series of 2-D images along the optical axis. However, resolution is always poorer along the optical axis than along the transversal axis because of the wave-like nature of light and limited numerical aperture (NA) of the objective lens. Confocal laser scanning microscopy is one of the most widely used techniques to improve axial resolution to observe 3-D structures in cells. Optical sectioning by confocal microscope is achieved using a small pinhole to exclude the out-of-focus light. However, the resolution is anisotropic, since the resolution along the optical axis is degraded roughly three-fold relative to the transverse resolution.[1] There are also other sophisticated techniques being developed to improve the resolution, such as interference and structured illumination methods,[2–4] and stimulated emission depletion microscopy (STED).[5] The powerful key to these high resolution microscopes is the imaged fluorescent dye itself.[6] However, these new techniques in high resolution fluorescence microscopy are not accessible for the current needs of cytopathologists, who rely on absorption-based stains. The cytopathologists currently make diagnoses based on a series of 2-D images acquired by a wide-field microscope.

Optical projection tomography has demonstrated 3-D images of large multicellular specimens such as embryos using low NA optics.[7] The optical projection tomography microscope (OPTM) is a newly developed instrument that can provide 3-D images of single cells with isometric high resolution both in fluorescence and absorption modes.[8,9] Although the depth of field of high NA objective lenses is small, we can scan the focal plane of the objective axially through the cell to acquire a focus-invariant image over a range many times greater than the depth of field.[8] We refer to this focus-invariant image as a "pseudoprojection." A custom microcapillary tube-based rotation stage allows a full 360 deg view of

Address all correspondence to: Qin Miao, University of Washington, Department of Bioengineering, 204 Fluke Hall, Seattle, Washington 98195. Tel: 206-883-5180; Fax: 206-685-8047; E-mail: miaoq@u.washington.edu.

1083-3668/2009/14(6)/064035/6/$25.00 © 2009 SPIE

the sample. Pseudoprojection images are taken from different perspectives by rotating the samples. After the acquisition of all pseudoprojection images, 3-D reconstruction is computed by using filtered backprojection, the standard method from x-ray computed tomography (CT).

A recent study shows that automated cell classification based on OPTM 3-D images provides advantages relative to classification performance based on 2-D images.[10] 3-D images can provide a dimension of depth, e.g., lines in 2-D images become surfaces in 3-D images, which can lead to additional 3-D features not available in 2-D. Features are unambiguously observed in 3-D images, since 3-D images are free of influence of orientation and focal plane selection. In single perspective images, optically dense parts can interfere with imaging of other parts further from the objective. This problem is minimized in OPTM, since the sample is viewed from different perspectives. In slide-based conventional microscopy, samples adhere to a flat glass slide, which can introduce morphological distortions. In OPTM, the samples are suspended in gel, so their original shapes can be conserved. Possibly due to these features of the OPTM, the resulting 3-D images of single cells provided by OPTM offer a three-fold reduction in false negative rate for adenocarcinoma detection versus 2-D images with the same high specificity.[10]

Biomarkers offer potential for early cancer diagnosis. Most biomarkers are observed under fluorescence microscopy. Since OPTM can image samples in both absorption and fluorescence modes, the biomarker pattern and the morphological structure in 3-D can be obtained with isometric high resolution for the same sample. The quantitative information of the biomarker, such as the concentration and distribution inside the cell, will add more features to the cancer diagnosis, which will consequently improve the sensitivity of the early cancer diagnosis. At the same time, the gold standards provided by the morphological features can validate the potential of new biomarkers for the diagnosis, since the cytopathologists have built a knowledge base for disease diagnosis based on more than 100 years of absorption images correlated to clinical outcomes.

In this work, the instrumentation and major components of a dual-modal microscope are described. Preliminary images of sample cells demonstrate that the 3-D images of absorption in transmission and fluorescence in epi-illumination are in coregistration.

2 Methods

2.1 *Optical Design*

The schematic of the OPTM is shown in Fig. 1. The sample stage is a custom-designed microcapillary tube-based rotation stage. The inner diameter of the microcapillary is 50 μm. It rotates in an oil-filled space between two flat, parallel glass surfaces (the two glass plates are not shown in Fig. 1). The cells are mixed with optical gel and injected into the microcapillary by a syringe. The optical gel, immersion oil, two glass plates, and the microcapillary have the same refractive index in the wavelength range used in this experiment. A high numerical aperture objective lens (100×, NA 1.3) is seated on a piezoelectric transducer (PZT) positioner. The PZT positioner (NV40/1CL, Piezosystem Jena, Jena, Germany) drives the objective to axially scan to get the pseudoprojection images. An 8-Hz triangular wave voltage is applied to PZT. Scanning range is adjusted for each sample to cover the entire sample during scanning. The scanning ranges used in this work for A549 cells and muntjac cells are 12 and 25 μm. 500 pseudoprojection images are taken at uniform angular intervals (0.72 deg) during one full rotation for both absorption (first rotation) and fluorescence (second rotation) for the same sample. One full rotation takes about one minute. OPTM can image in both fluorescence and absorption modes using the same objective. A mercury arc lamp provides epi-illumination for the fluorescence mode and a quartz-tungsten-halogen (QTH) lamp provides transmission illumination for the absorption mode. A bandpass filter (D585/60×, Chroma, Vemont) is put in the transmission illumination path to limit the wavelength around 600 nm. Hematoxylin dye has an absorption peak near 600 nm, so this filter can improve the image contrast for hematoxylin-stained cells. At the same time, this filter can prevent unnecessary photobleaching during imaging in the absorption mode, because the filtered light is beyond the excitation wavelength of the fluorophores used in this experiment.

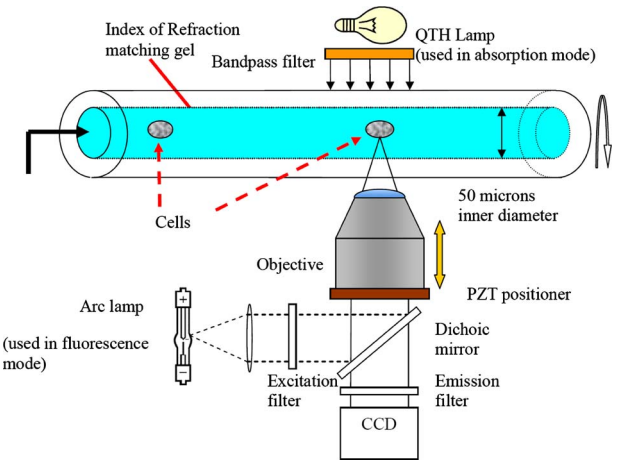

Fig. 1 Schematic of the optical projection tomography microscope.

2.2 *Image Processing*

500 pseudoprojection images were taken for each sample in absorption mode as well as in fluorescence mode. Because vibrations can cause the misalignment of the pseudoprojection images, the center of mass of each pseudoprojection is identified and aligned to correct for registration errors. Photobleaching can diminish the amount of fluorescent signal in fluorescence mode. The optical density signal inside the sample can be described as the "mass" of the sample. The mass corresponds to the total number of fluorescence emitters in the sample. The principle of mass conservation is adapted here to correct for this error. Figure 2(b) shows a fluorescently labeled chromosome. Figures 2(a) and 2(c) plot the intensity profiles of the two orthogonal projections of the object. The area beneath the curve in Figs. 2(a) and 2(c) corresponds to the total signal (mass) of the object in Fig. 2(b). Although the shapes of the curves are different, the area beneath the curves should be the same according to the principle of mass conservation. In OPTM, the sum of intensities in each pseudoprojec-

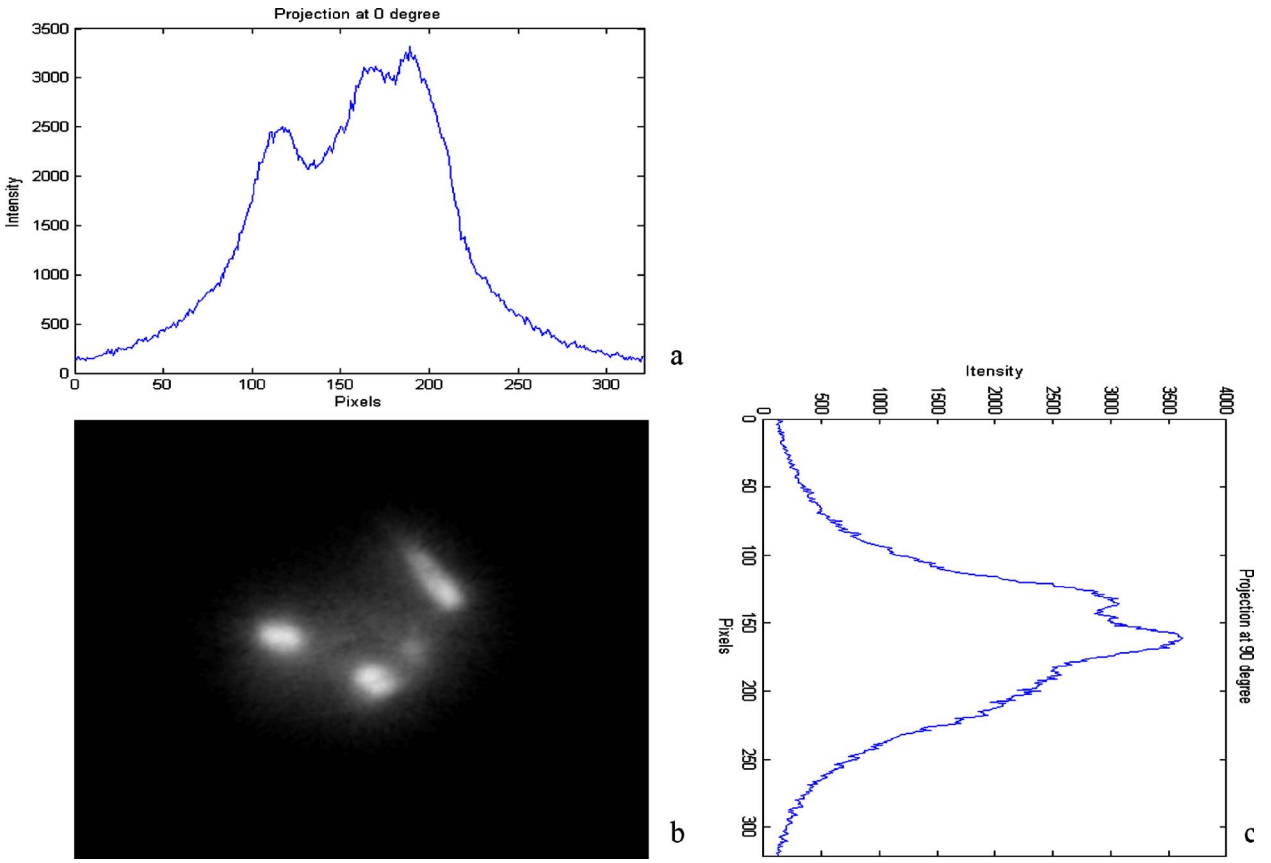

Fig. 2 (a) and (c) show the intensity profile as image (b) is projected onto two orthogonal directions.

tion should be the same if there is no photobleaching, since it corresponds to the total signal of the sample. Here, we assume that the photobleaching rate of fluorophores was uniform spatially throughout the volume. Based on this, the sum of the intensities in the first pseudoprojection is calculated. Correction factors for the following pseudoprojection images are obtained by normalizing the subsequent pseudoprojection images to this initial pseudoprojection value. After corrections are applied to all pseudoprojections, filtered backprojection is applied for the tomographic reconstruction.[11] The resulting reconstructed slices are imported into the VolView visualization utility (Kitware Incorporated, New York). In VolView, a crosssection is cropped from whole 3-D images. Opacity mapping is done to map the histogram to opacity. Two thresholds are found: one to separate the background from the cell, the other to separate the cytoplasm from the chromosome. Opacity of the background is set to zero. The part that has a grayscale value larger than the second threshold is considered the chromosome. Opacity of the chromosome is set to 1 and this part is also colored. The opacity of the cytoplasm is set to a value between 0 and 1.

2.3 *Sample Preparation*

Female Indian muntjac cells were a gift of Schultz (Signature Genomic Laboratories, Spokane, Washington). Muntjac cells were treated with colchicine (D1925, Sigma, Saint Louis, Missouri) to arrest cells in metaphase. Acetic acid methanol (1:3) was used to fix muntjac cells. The muntjac cells are first stained with hematoxylin (Gill's hematoxylin Number 1, Electron Microscopy Sciences, Hatfield, Pennsylvania). Then after washing in HEPES buffer, the cells are incubated in Sytox Green solution (1/5000 dilution from stock, stock concentration: 5 mM, Invitrogen, Carlsbad, California). Cells were then washed again in HEPES, dehydrated in alcohols, cleared in xylene, and embedded in optical gel for imaging. For coregistration measurement, cultured adenocarcinoma cells (A549) are used. Cells are first fixed in 4% formaldehyde, then stained with hematoxylin (Gill's hematoxylin Number 1, Electron Microscopy Sciences, Hatfield, Pennsylvania).

3 Results

3.1 *Tomographic Simulation for Point Object*

We simulated the image of a point object in both a bright-field microscope and OPTM to demonstrate how OPTM improves the resolution along the optical (axial) axis. The 3-D image of the point object in a bright-field microscope is simply the point spread function (PSF) of the objective.[12] Objective specifications used in the simulation are the same as in the experiments: 100×, NA 1.3, and refractive index of immersion oil: 1.516. The pseudoprojection image for OPTM is calculated as the projection of the PSF for bright-field microscopes along the optical axis. Then the reconstructed images of the point object are calculated using these pseudoprojection images. Figure 3(a) shows the axial section of the PSF in

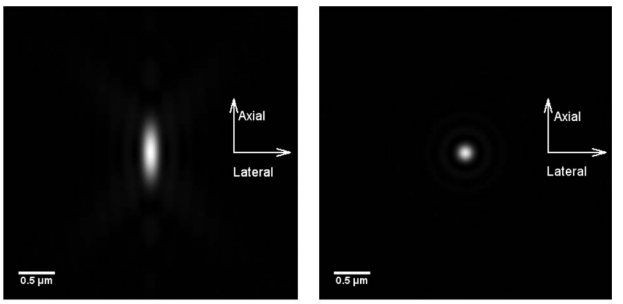

Fig. 3 (a) Image of point object in the axial section in a bright-field microscope calculated for objective, 100×/NA 1.3. (b) Image of point object in the axial section in OPTM.

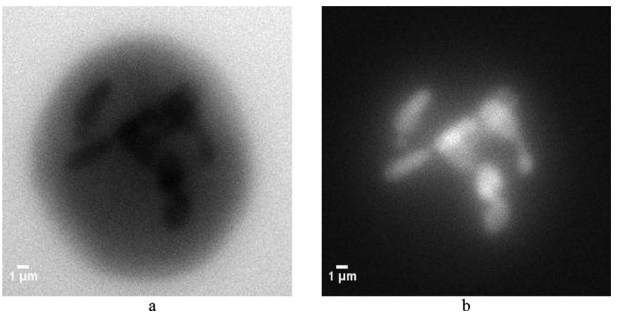

Fig. 5 Pseudoprojection images of one cell (female Indian muntjac cell arrested in metaphase) in (a) absorption mode and (b) fluorescence mode.

bright field. We can see that the axial resolution is poorer than the lateral resolution. Since OPTM can use the lateral resolution from one view to compensate for the poor axial resolution from another view, isometric high resolution can be obtained. Figure 3(b) shows the axial section of PSF in OPTM. By comparing Figs. 3(a) and 3(b), we can see that OPTM can provide isometric resolution along all axes.

3.2 *Experimentally Measured Point Spread Function of an Optical Projection Tomography Microscope*

Fluorescent microspheres (TransFluoSpheres, Invitrogen, Carlsbad, California) are used here to measure the point spread function. The excitation maximum is 488 nm, and the emission maximum is 560 nm. The mean diameter of the microspheres is 100 nm. The reconstructed images are interpolated to make the images look smooth. Figure 4(a) shows the axial section of the PSF. The axial direction is parallel to the optical axis of the objective. The normalized intensity profiles along lateral and axial directions are shown in Figs. 4(b) and 4(c). Full width at halfmaximum (FWHM) is considered as the spatial resolution along each axis. The resulting lateral and axial resolution measured from the reconstructed images are both 0.35 μm.

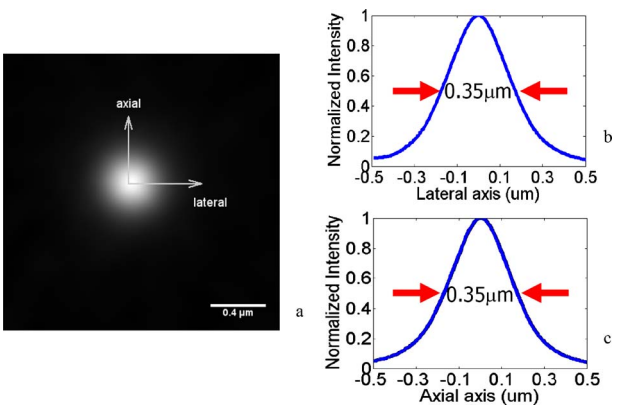

Fig. 4 Fluorescence microsphere with a diameter of 100 nm was imaged using 488-nm excitation. Since the size of the microsphere is well below the resolution, the reconstructed image of the microsphere is used as a measure of point spread function: (a) Axial section of point spread function; (b) normalized intensity profile along the lateral direction; and (c) normalized intensity profile along the axial direction.

3.3 *Imaging of Biological Samples*

Female Indian muntjac cells were treated with colchicine to arrest cells in metaphase to make the six large chromosomes visible. Then cells are then stained with hematoxylin (absorption stain) and Sytox Green (fluorescence stain). Figure 5(a) shows one pseudoprojection image in absorption mode; Fig. 5(b) shows one pseudoprojection image in fluorescence mode.

3-D reconstructed images from both absorption and fluorescence modes for the same cell are shown in Video 1. Two snapshot images from two different perspectives are displayed in Fig. 6. The female Indian muntjac cell has six large chromosomes, which can be easily distinguished in the reconstructed images in both imaging modes in 3-D.

4 Discussion

In this study, 3-D images of the same dual-labeled cell with high isometric resolution in both absorption and fluorescence modes are shown. In the experiment, absorption pseudoprojection images are taken in the first rotation, and fluorescence pseudoprojection images are taken in subsequent rotation. Mechanical error can cause the misalignment of the two datasets. To verify the coregistration between the two pseudoprojection sets, we use the phase correlation method[13] to find the matching images in both modes. Each time, we

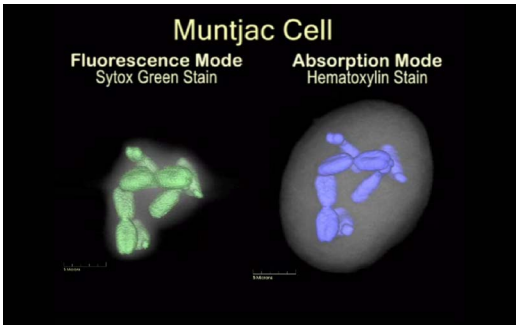

Video 1 3-D reconstructed images of a muntjac cell that is arrested in metaphase are shown (QuickTime, 909.54 KB).
[URL: http://dx.doi.org/10.1117/1.3275470.1].

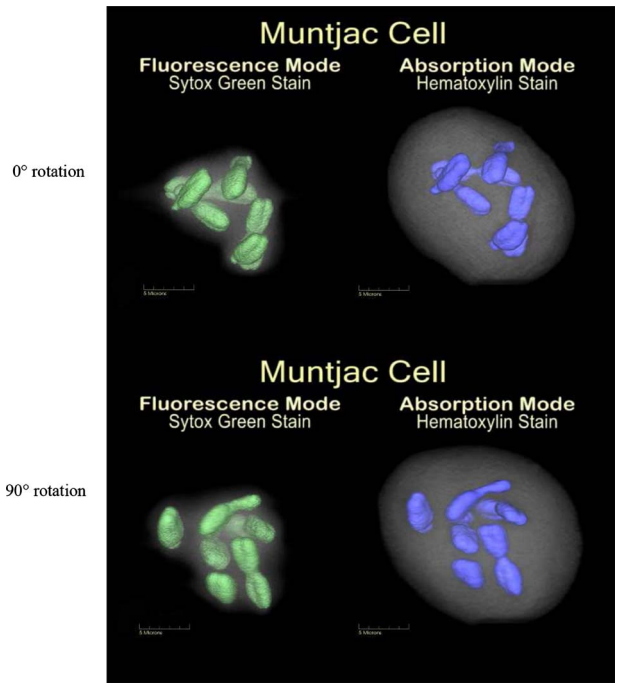

Fig. 6 3-D reconstruction of a female Indian muntjac cell that is arrested in metaphase. Left is the fluorescence image, right is the absorption image.

take one pseudoprojection from the fluorescence mode, then calculate the phase correlation function between this image and each of the images from the absorption mode. The image in the absorption mode that gives the highest peak is considered the best matching image. The best matching images and the corresponding fluorescence images are plotted in Fig. 7. The blue curve is the original data and the red curve is the best-fit line. The slope of the line is 1, which implies that we have good matching between the fluorescence and absorption data. To quantitatively measure the coregistration error between the 3-D reconstructed images from two different rotations, two 3-D reconstructed images of the same cell are compared. Two pseudoprojection sets of hematoxylin-stained cells are taken in two different rotations. 3-D images are reconstructed using the backprojection algorithm. Since we use the same exact cell in the two rotations, the only error that can cause the misalignment of the 3-D images is the mechanical error. We quantitatively measure this misalignment by using the phase correlation method. This misalignment can be considered as a quantitative estimation of the mechanical error. The misalignment between the two 3-D images is measured to be within one pixel. The pixel size in our images is 76 nm, so the mechanical error in the system is estimated to be within the resolution of the system, which is 350 nm.

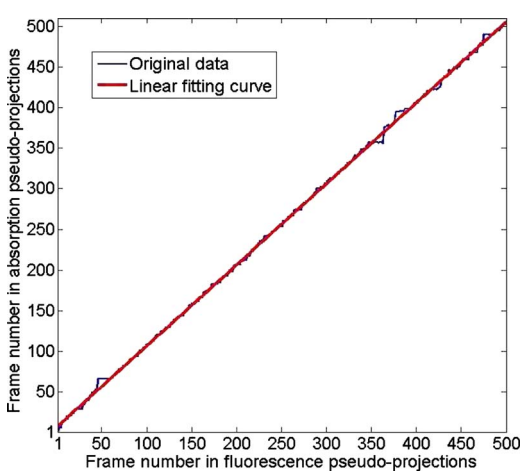

Fig. 7 Phase correlation method is used to find the best-matching images in absorption pseudoprojections for each image in the fluorescence pseudoprojections. (Color online only.)

Trial No.	3D correlation coefficients between trial #1 and trial #2-5 for each cell			
	Cell #1	Cell #2	Cell #3	Cell #4
1				
2	0.9998	0.9997	0.9996	0.9991
3	0.9994	0.9993	0.9992	0.9980
4	0.9996	0.9990	0.9996	0.9988
5	0.9993	0.9984	0.9991	0.9978
Mean	0.9995	0.9991	0.9994	0.9984
Standard deviation	0.0002	0.0005	0.0003	0.0006

Fig. 8 Instrument repeatability measurements summary. Each of the four cells was imaged five times consecutively. The 3-D similarity between the reconstructed images in the first trial and the four following trials is measured by 3-D correlation coefficients, which are listed. For cell 4, one slice from each of the five trials at the same position is shown in the last column.

Instrument repeatability was tested by taking images of one hematoxylin-stained cell five times consecutively. The 3-D similarity between the reconstructed images in the first trial and the following four trials for the same cell is measured by the 3-D correlation coefficient.[14] We repeated this experiment for four different cells and the results are summarized in Fig. 8. Slices from each of the five different trials for the one cell (4) having the lowest similarity measured by 3-D the correlation coefficient are also shown in Fig. 8. The results show that the instrument can preserve cell features well in repeated optical scans, as the repeated images of cell 4 are indistinguishable by an experienced human observer.

In Fig. 6, the cytoplasm of the cell in absorption mode can be easily distinguished. However, in fluorescence mode only the cytoplasm near the large chromosomes can be clearly seen. In absorption mode, a small residue of hematoxylin is assumed to be distributed throughout the cytoplasm, which allows the cytoplasm membrane to be distinguished. Since RNA concentration in the cytoplasm is very low, the signal from the cytoplasm is expected to be quite weak in the fluorescence mode. As a result, the entire cytoplasm cannot be distinguished from the background. The halos around chromosomes in the fluorescence mode can be caused by the scattering of light emitted from the labeled chromosomes.

As mentioned in Sec. 2.3, muntjac cells are first stained with hematoxylin and then with Sytox Green. The order of staining is important. Hematoxylin solution's high pH may affect Sytox Green's ability to fluoresce. Sytox Green can be sensitive to the ionic and polarity environment provided by hematoxylin solution. At the same time, exposure to light can cause photobleaching if fluorescence dye is added prior to absorption staining.

5 Conclusion

The practice of clinical cytology relies mostly on bright-field microscopy using absorption stains, while the practice of molecular biology research relies on fluorescence microscopy and molecular probes. OPTM allows 3-D imaging of both contrast mechanisms with isometric high resolution of 0.35 μm, which makes it a valuable tool for both disease diagnosis and biological research.

Acknowledgment

The authors thank Roger A. Schultz and Lisa D. McDaniel, Signature Genomic Laboratories, Spokane, Washington, for providing Indian muntjac cells; Ben Hawthorne for helping with sample preparation; and David Steinhauer for helping with image processing. Gift funding is provided by VisionGate Incorporated to Eric J. Seibel.

References

1. T. Wilson, *Confocal Microscopy*, Academic Press, San Diego, California (1990).
2. M. G. L. Gustafsson, D. A. Agard, and J. W. Sedat, "I5M: 3D widefield light microscopy with better than 100 nm axial resolution," *J. Microsc.* **195**, 10–16 (1999).
3. M. Schrader and S. W. Hell, "4Pi-confocal images with axial superresolution," *J. Microsc.* **183**, 189–193 (1996).
4. M. Neil, R. Juskaitis, and T. Wilson, "Method of obtaining optical sectioning by using structured light in a conventional microscope," *Opt. Lett.* **22**, 1905–1907 (1997).
5. V. Westphal, I. Kastrup, and S. W. Hell, "Lateral resolution of 28 nm in far-field fluorescence microscopy," *Appl. Phys. B* **77**, 377–380 (2003).
6. S. W. Hell, "Microscopy and its focal switch," *Nat. Methods* **6**, 24–32 (2009).
7. J. Sharpe, U. Ahlgren, P. Perry, B. Hill, A. Ross, J. Hecksher-Sorensen, R. Baldock, and D. Davidson, "Optical projection tomography as a tool for 3D microscopy and gene expression studies," *Science* **296**, 541–545 (2002).
8. M. Fauver, E. J. Seibel, J. R. Rahn, M. G. Meyer, F. W. Patten, T. Neumann, and A. C. Nelson, "Three-dimensional imaging of single isolated cell nuclei using optical projection tomography," *Opt. Express* **13**, 4210–4233 (2005).
9. Q. Miao, J. R. Rahn, R. C. Bryant, C. A. Lancaster, A. Tourovskaia, T. Neumann, E. J. Seibel, and A. C. Nelson, "Multimodal three-dimensional imaging with isometric high resolution using optical projection tomography," *Proc. SPIE* **7262**, 72620V (2009).
10. M. Meyer, M. Fauver, J. R. Rahn, T. Neumann, F. W. Patten, E. J. Seibel, and A. C. Nelson, "Automated cell analysis in 2D and 3D: a comparative study," *Pattern Recogn.* **42**, 141–146 (2009).
11. A. C. Kak and M. Slaney, *Principles of Computerized Tomographic Imaging*, IEEE Press, New York (1988).
12. M. Gu, *Advanced Optical Imaging Theory*, Springer Verlag, Berlin (2000).
13. E. De Castro and C. Morandi, "Registration of translated and rotated images using finite Fourier transforms," *IEEE Trans. Pattern Anal. Mach. Intell.* **PAMI-9**, 700–703 (1987).
14. J. S. Suri, D. L. Wilson, and S. Laxminarayan, *Handbook of Biomedical Image Analysis: Registration Models*, Kluwer Academic/Plenum Publishers, New York (2005).